Disrupted mechanical stability of the dystrophin-glycoprotein complex causes severe muscular dystrophy in sarcospan transgenic mice

Angela K. Peter[1,*], Gaynor Miller[1,*] and Rachelle H. Crosbie[1,2,‡]

[1]Department of Physiological Science and [2]Molecular Biology Institute, University of California, Los Angeles, CA 90095, USA

*These authors contributed equally to this work

‡Author for correspondence (e-mail: rcrosbie@physci.ucla.edu)

Accepted 23 November 2006
Journal of Cell Science 120, 996-1008 Published by The Company of Biologists 2007
doi:10.1242/jcs.03360

Summary

The dystrophin-glycoprotein complex spans the muscle plasma membrane and provides a mechanical linkage between laminin in the extracellular matrix and actin in the intracellular cytoskeleton. Within the dystrophin-glycoprotein complex, the sarcoglycans and sarcospan constitute a subcomplex of transmembrane proteins that stabilize α-dystroglycan, a receptor for laminin and other components of the extracellular matrix. In order to elucidate the function of sarcospan, we generated transgenic mice that overexpress sarcospan in skeletal muscle. Sarcospan transgenic mice with moderate (tenfold) levels of sarcospan overexpression exhibit a severe phenotype that is similar to mouse models of laminin-deficient congenital muscular dystrophy (MD). Sarcospan transgenic mice display severe kyphosis and die prematurely between 6 and 10 weeks of age. Histological analysis reveals that sarcospan expression causes muscle pathology marked by increased muscle fiber degeneration and/or regeneration. Sarcospan transgenic muscle does not display sarcolemma damage, which is distinct from dystrophin- and sarcoglycan-deficient muscular dystrophies. We show that sarcospan clusters the sarcoglycans into insoluble protein aggregates and causes destabilization of α-dystroglycan. Evidence is provided to demonstrate abnormal extracellular matrix assembly, which represents a probable pathological mechanism for the severe and lethal dystrophic phenotype. Taken together, these data suggest that sarcospan plays an important mechanical role in stabilizing the dystrophin-glycoprotein complex.

Key words: Muscular dystrophy, Dystrophin, Dystrophin-glycoprotein complex, Sarcospan

Introduction

The dystrophin-glycoprotein complex (DGC) is located at the muscle plasma membrane and provides a critical linkage between the extracellular matrix and the cytoskeleton (Campbell and Kahl, 1989; Ervasti and Campbell, 1991; Ervasti and Campbell, 1993; Ervasti et al., 1991; Ervasti et al., 1990; Yoshida and Ozawa, 1990). Sarcospan, a 25-kDa transmembrane protein, is the most recently identified component of the dystrophin-glycoprotein complex (Crosbie et al., 1997; Crosbie et al., 1998). Sarcospan (SSPN) interacts with the sarcoglycans (SGs) to form a tight subcomplex within the DGC (Crosbie et al., 1999). The SGs are a group of single-pass transmembrane glycoproteins (α-, β-, γ- and δ-SG) (Bonnemann et al., 1995; Jung et al., 1996; Lim et al., 1995; McNally et al., 1994; Nigro et al., 1996; Roberds et al., 1993; Roberds et al., 1994). In addition to the SG-SSPN subcomplex, the other components of the DGC include dystrophin, syntrophin and the dystroglycans (α- and β-DG) (Adams et al., 1993; Hoffman et al., 1987; Ibraghimov-Beskrovnaya et al., 1992; Yang et al., 1994). α-DG is a receptor for proteins in the extracellular matrix, including laminin, agrin, perlecan and neurexin (for a review, see Michele and Campbell, 2003). Genetic mutations in many of the genes encoding components of the DGC result in a variety of muscular dystrophies (for a review, see Durbeej and Campbell, 2002). Mutations in the dystrophin gene are responsible for X-linked Duchenne muscular dystrophy (MD), which is characterized by progressive muscle weakness and loss of the entire DGC from the sarcolemma (for a review, see Durbeej and Campbell, 2002). Mutations in the SGs cause autosomal recessive limb girdle muscular dystrophies (AR-LGMD) 2C-2F. In most cases of sarcoglycan-deficient AR-LGMD, the entire SG-SSPN subcomplex is lost from the sarcolemma (for a review, see Dalkilic and Kunkel, 2003).

The function of the SG-SSPN subcomplex is to stabilize α-DG at the sarcolemma (Duclos et al., 1998; Durbeej et al., 2000; Holt et al., 1998; Straub et al., 1998), thereby completing the linkage between the extracellular matrix and the F-actin cytoskeleton (Ervasti and Campbell, 1993). Disruption of this linkage renders the sarcolemma susceptible to contraction-induced damage (Petrof et al., 1993). SSPN is absent from the sarcolemma of patients with sarcoglycan-deficient AR-LGMD, indicating that membrane targeting and stability of SSPN is dependent on the SGs (Crosbie et al., 1999). Sarcospan is not restored to the sarcolemma even in AR-LGMD cases with partial SG deficiency where three out of four

SGs are expressed (Crosbie et al., 1999). Taken together, these data support a role for expression of the *complete* SG-SSPN subcomplex to prevent MD.

The precise function of SSPN within the DGC has been elusive. SSPN-deficient mice maintain normal muscle function and do not exhibit perturbation of the DGC (Lebakken et al., 2000). One possible conclusion from this work might be that SSPN is not a critical component of the DGC and does not contribute to muscle function. However, this conclusion may be premature since it is unknown whether another protein replaces the function of SSPN in SSPN-null mice. As a tetraspanin-like protein, SSPN is poised to play a critical structural role within the DGC. Tetraspanins possess four transmembrane domains, a small intracellular loop and a larger extracellular loop. The primary function of tetraspanins is to organize proteins at the plasma membrane (for reviews, see Hemler, 2003; Levy and Shoham, 2005). By mediating interactions between transmembrane proteins within the plane of the membrane, tetraspanins play important roles in cell adhesion, motility and signaling (for a review, see Hemler, 2001).

In the current study, we engineered transgenic mice to overexpress SSPN protein in skeletal muscle as an alternate approach to investigate the function of SSPN. SSPN transgenic (SSPN-Tg) mice exhibit a severe phenotype that is much more similar to laminin-deficient muscle (Besse et al., 2003; Guo et al., 2003; Kuang et al., 1998; Miyagoe et al., 1997; Sunada et al., 1994; Xu et al., 1994). Taken together, our data support a necessary role for SSPN in organizing proteins within the DGC and in assembly of the extracellular matrix.

Results

Skeletal muscle expression of SSPN causes lethality and severe muscle pathology

As an approach to investigate the function of SSPN, we introduced SSPN cDNA into mice in order to create SSPN transgenic mice (SSPN-Tg). The SSPN transgene was engineered by placing the full-length human SSPN cDNA sequence (hSSPN) under control of the human skeletal α-actin promoter, which limits transgene expression to skeletal muscle tissues (Fig. 1A). In order to distinguish between endogenous and heterologous SSPN expression, the transgene was designed using SSPN cDNA from human. In our studies to examine the biochemical properties of SSPN, we find that human SSPN behaves identically to mouse SSPN. Although we cannot exclude the possibility that human SSPN has an additional, unknown function separate from mouse SSPN, we believe that the overwhelming biochemical similarities between human, rabbit, and mouse SSPN (Crosbie et al., 1997; Crosbie et al., 1998) support a similar role for each of these proteins in their respective species. Although human and mouse SSPN are ~90% identical (Crosbie et al., 1997), small amino acid variations in the N- and C-terminal regions permitted generation of antibodies specific to exogenous (human) and endogenous (mouse) SSPN (Miller et al., 2006). Five lines of SSPN-Tg mice (29.1, 31.6, 36.6, 31.7, and 37.5) were analyzed for SSPN transgene expression by immunoblot analysis of total muscle lysates. Although McNally and colleagues reported the isolation of several γ-SG transgenic mice with 150-times more γ-SG relative to endogenous levels (Zhu et al., 2001), we never identified transgenic mice with greater than tenfold SSPN protein expression. This suggests that high levels of SSPN may be toxic. Of the five independent founder lines chosen for further analysis, two SSPN transgenic expressers (lines 31.7 and 37.5) were significantly smaller than their wild-type, non-Tg controls, as illustrated in representative photographs (Fig. 1B). SSPN protein was expressed at levels approximately tenfold over non-Tg controls (Fig. 4). The phenotypic SSPN-Tg mice appeared atrophic and less mobile than their non-Tg littermates. Furthermore, phenotypic SSPN-Tg mice displayed severe kyphosis (Fig. 1B), weighed 50% less than age-matched, non-Tg controls (Fig. 1C), and died prematurely between 6 and 10-weeks of age (data not shown). Non-phenotypic SSPN-Tg lines 29.1, 31.6, and 36.6 expressed lower levels of SSPN protein (approximately two- to sixfold) and were indistinguishable from their non-Tg controls (data not shown).

Histological analysis of quadriceps, tibialis anterior, soleus and diaphragm muscles was performed on phenotypic and non-phenotypic SSPN-Tg muscle using Hematoxylin and Eosin staining. In comparison to non-Tg controls, only the phenotypic SSPN-Tg muscle displayed pathology characterized by myofiber fibrosis, central nucleation and variation in fiber size (Fig. 2A). In comparison to non-Tg

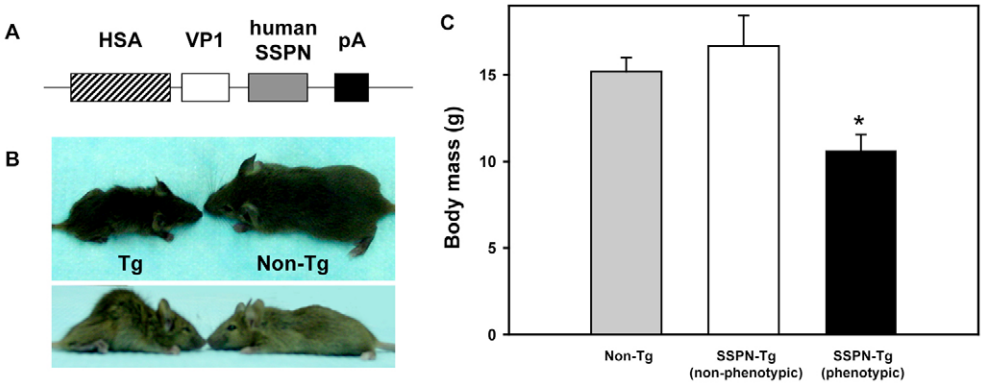

Fig. 1. SSPN-Tg mice display kyphosis and reduced body mass. (A) Schematic diagram of construct used to generate SSPN-Tg mice. A human skeletal muscle α-actin promoter (HSA) was used to control muscle-specific expression of the human SSPN (hSSPN) transgene. A SV40 VP1 intron serves as a splice acceptor and is located downstream of the HSA promoter. Polyadenylation sites (pA) were inserted at the 3′ end of the hSSPN cDNA. (B) Representative photographs of phenotypic Tg and non-Tg littermates reveal dramatic differences in body size and length. Severe kyphosis is evident in the phenotypic Tg mouse, as illustrated in the side view. Phenotypic SSPN-Tg mice appear atrophic and have limited mobility. Non-phenotypic SSPN-Tg mice were indistinguishable from their non-Tg controls (data not shown). (C) Phenotypic SSPN-Tg mice are nearly 50% lighter than non-Tg controls. Body mass (g) of 4-week-old non-Tg (n=14), non-phenotypic SSPN-Tg (n=3), and phenotypic SSPN-Tg (n=5) is plotted. Values are means and s.e.m.; *P=0.0015.

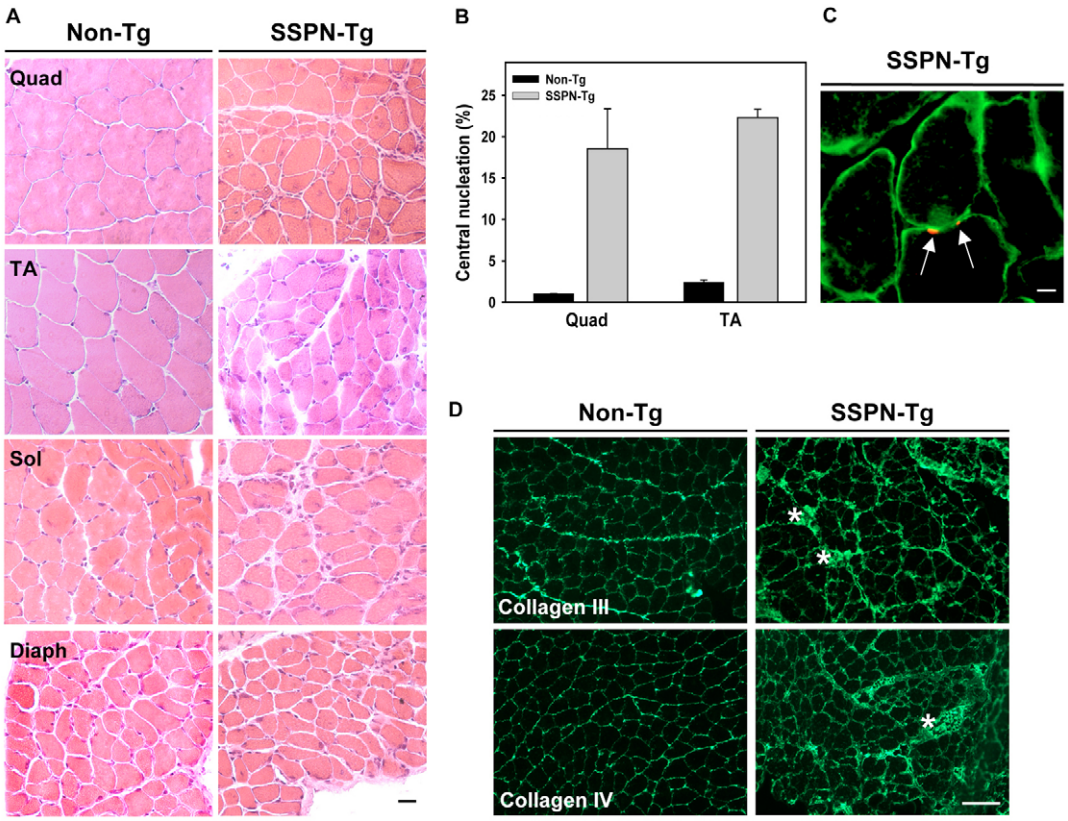

Fig. 2. SSPN-Tg mice display muscle pathology. (A) Transverse cryosections of quadriceps (Quad), tibialis anterior (TA), soleus (Sol), and diaphragm (Diaph) muscles from non-Tg and phenotypic SSPN-Tg (line 37.5) mice were stained with Hematoxylin and Eosin. SSPN-Tg muscle exhibits a greater variation in fiber diameter in comparison to non-Tgs. Pathological features were not observed in non-phenotypic SSPN-Tg muscle (data not shown). Bar, 20 μm. (B) Central nucleation (%) was quantified for quadriceps and tibialis anterior muscles isolated from 4-week-old phenotypic SSPN-Tg mice and non-Tg littermate controls. SSPN-Tg mice display between 17- and 20-fold more fibers with centrally placed nuclei compared to non-Tgs. Values are means and s.e.m. of total fibers counted. *$P \leqslant 0.05$. (C) DNA fragmentation was analyzed by TdT-dUTP labeling. Apoptotic myonuceli (red, arrows) were present only in phenotypic SSPN-Tg mice and were never observed in non-Tg or non-phenotypic SSPN-Tg. Both apoptotic nuclei shown lie within the same myofiber outlined with β-DG (green). Bar, 50 μm. (D) Quadriceps muscle from non-Tg and phenotypic SSPN-Tg mice was stained with antibodies to collagen III and collagen IV. Small areas of fibrosis in the SSPN-Tg muscle are denoted with an asterisk. Bar, 20 μm.

controls, phenotypic SSPN-Tg mice displayed 15- and 20-fold more central nucleation in quadriceps and tibialis anterior muscles, respectively (Fig. 2B). Diaphragm muscles appeared relatively normal as a result of the low levels of transgene expression in this muscle. Previous results have shown that disruption of the interaction between α-dystroglycan and the extracellular matrix protein laminin induces apoptosis in muscle cells (Langenbach and Rando, 2002). In order to assess if possible disruption between the extracellular matrix and the DGC causes apoptosis in phenotypic SSPN-Tg mice, we performed TUNEL staining of skeletal muscle cryosections. Increased DNA fragmentation was noted in phenotypic SSPN-Tg mice but was absent in non-Tg controls and non-phenotypic SSPN-Tg mice (arrows, Fig. 2C). Small areas of fibrosis characterized by patches of collagen-III and collagen-IV accumulation were evident in the phenotypic SSPN-Tg muscle (asterisks, Fig. 2D), but not in non-Tg controls.

Sarcolemma integrity is not compromised by SSPN overexpression

Dystrophin- and sarcoglycan-deficient muscular dystrophies are characterized by sarcolemma instability, as illustrated by the unregulated exchange of molecules between the circulating blood serum and the muscle fiber (Coral-Vazquez et al., 1999; Duclos et al., 1998; Durbeej et al., 2000; Menke and Jockusch, 1991; Petrof et al., 1993; Straub et al., 1997; Weller et al., 1990). We analyzed membrane integrity in SSPN-Tg mice using two established methods. First, an Evans Blue tracer assay was performed to examine the presence of blood serum proteins in myofibers (Matsuda et al., 1995; Straub et al., 1997). Evans Blue is a fluorescent dye that binds to albumin in the serum and accumulates in the cytosol of damaged muscle fibers, presumably by entering through unrepaired tears in the membrane (Matsuda et al., 1995; Straub et al., 1997). Evans Blue dye accumulation was analyzed in quadriceps muscle fibers after introduction of the tracer by i.p. injection into SSPN-Tg and non-Tg mice. Muscle from phenotypic SSPN-Tg mice was negative for Evans Blue dye uptake (Fig. 3A). Muscle from injected *mdx* mice is shown as a positive control (Fig. 3A). No Evans Blue-positive fibers were found in non-phenotypic SSPN-Tg mice (data not shown).

As a second method, we evaluated the leakage of muscle-

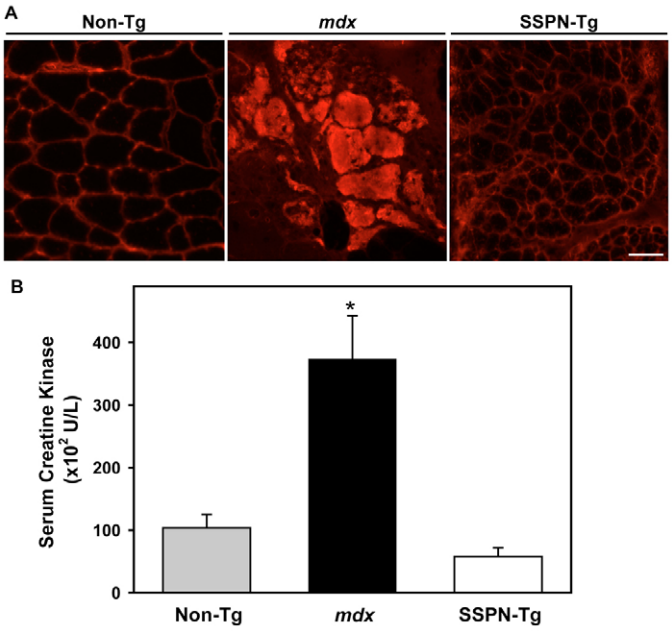

Fig. 3. SSPN-Tg mice do not exhibit sarcolemma instability. (A) Evans Blue tracer assay for infiltration of blood serum proteins into the muscle fiber. Intraperitoneal injection of Evans Blue dye can be detected in muscle fibers with damaged sarcolemma. Transverse cross sections of quadriceps muscle were imaged using a fluorescence microscope equipped with green activation filters. An image from *mdx* muscle, which has severe membrane damage, is shown as a positive control for Evans Blue staining. Evans Blue dye was not detected in phenotypic or non-phenotypic (data not shown) SSPN-Tg mice. Bar, 50 μm. (B) Analysis of muscle-specific creatine kinase in circulating blood serum. Creatine kinase activities were evaluated in serum samples from non-Tg, *mdx*, and phenotypic SSPN-Tg mice. SSPN-Tg mice do not exhibit leakage of muscle-specific creatine kinase into the blood serum. Values are means and s.e.m. of total mice analyzed. **P*=0.002 compared to control.

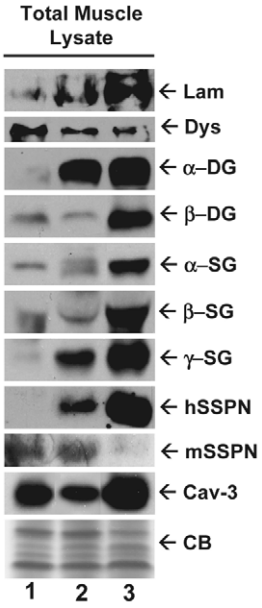

Fig. 4. DGC proteins are increased upon SSPN overexpression. Immunoblot analysis of total proteins extracted from skeletal muscle of non-Tg (lane 1), non-phenotypic SSPN-Tg line 29.1 (lane 2), and phenotypic SSPN-Tg line 37.5 (lane 3) mice. Skeletal muscle was solubilized using 3% SDS buffer and protein samples (60 μg) were separated by SDS-PAGE and transferred to nitrocellulose membranes. Equal loading of protein samples was confirmed by Coomassie Blue (CB) stain. Immunoblots were probed with antibodies to laminin (Lam), dystrophin (Dys), α- and β-DG, α-, β-, and γ-SG, exogenous SSPN (hSSPN), endogenous SSPN (mSSPN) and caveolin-3 (cav-3), as indicated.

specific creatine kinase (CK) into the blood serum (McArdle et al., 1994). Consistent with results from the Evans Blue tracer assay, serum levels of CK in phenotypic SSPN-Tg mice was similar to non-Tg littermate controls (Fig. 3B). The levels of serum CK from *mdx* mice is shown for comparison (Fig. 3B). Taken together, these data demonstrate that sarcolemma integrity is not altered upon SSPN overexpression, which is distinct from dystrophin- and sarcoglycan-deficient muscular dystrophies. This finding makes SSPN-Tg mice similar to laminin-defective mice, which also do not display significant membrane damage (Straub et al., 1997).

Upregulation of the DGC in SSPN-Tg mice

Our observation that SSPN-Tg mice display severe muscle pathology suggests that the DGC may be structurally or functionally altered. Immunoblots of skeletal muscle extracts from non-phenotypic and phenotypic SSPN-Tg mice were probed with antibodies to laminin (Lam), dystrophin (Dys), the DGs (α- and β-DG), the SGs (α- and γ-SG), mSSPN, hSSPN, and caveolin-3. With the exception of dystrophin and mSSPN, overexpression of the hSSPN transgene caused increased expression of the DGC components (Fig. 4). Quantification of immunoblots revealed that non-phenotypic SSPN-Tg muscle exhibits mildly increased levels of DGC protein. However, in phenotypic SSPN-Tg mice the expression of DGC proteins was higher. α-DG was upregulated by 9-fold and α-and β-SG levels were increased by fivefold relative to non-Tg controls. γ-SG levels were approximately tenfold greater in phenotypic SSPN-Tg when compared to non-Tgs. Caveolin-3 levels were increased by twofold in phenotypic SSPN-Tg mice.

Previous studies have shown that overexpression of γ-SG can cause mislocalization of the entire SG subcomplex (Zhu et al., 2001). In order to determine if SSPN induced similar effects on the DGC, we examined skeletal muscle cryosections from phenotypic SSPN-Tg and non-Tg mice. Indirect immunofluorescence with antibodies to α-and β-DG as well as α-, β- and γ-SG was more intense in SSPN-Tg muscle relative to non-Tg controls (Fig. 5). Exogenous, human SSPN (hSSPN), which is highly expressed at the sarcolemma, caused down regulation of endogenous, mouse SSPN (mSSPN) in SSPN-Tg mice (Fig. 5). This suggests that regulatory mechanisms are in place to control levels of SSPN protein expression. In agreement with immunoblot analysis, levels of dystrophin were decreased in SSPN-Tg mice (Fig. 5). Immunoblot analysis showed that laminin was elevated in both phenotypic and non-phenotypic SSPN-Tg mice (Fig. 4). However, the increased expression of laminin in phenotypic SSPN-Tg tissue resulted in large areas of laminin accumulation in the extracellular space (Fig. 5). Such aggregates were never observed in non-phenotypic SSPN-Tg mice (data not shown). Caveolin-3 staining was increased at the sarcolemma in SSPN-Tg skeletal muscle (Fig. 5), which is consistent with total protein levels (Fig. 4). Although overexpression of SSPN alters the total levels of protein expression, it does not perturb sarcolemma localization of any of the DGC components.

SSPN-mediated aggregation of the SG subcomplex

Tetraspanin-tetraspanin interactions within the plasma membrane form microdomains that cluster transmembrane proteins, thereby controlling a variety of cell functions. If SSPN does indeed behave as a tetraspanin, then SSPN-

mediated structures might serve as a scaffold for organization of the DGC. We hypothesized that overexpression of SSPN might cause formation of SSPN-SSPN aggregates within the sarcolemma, which might trap the DGC into insoluble protein aggregates that are resistant to detergent extraction. In order to determine whether SSPN expression caused aggregation of the DGC, proteins from SSPN-Tg muscle were separated into soluble and insoluble fractions after treatment with 1% digitonin (Fig. 6A). Both the soluble and insoluble pellet fractions were analyzed by immunoblotting with antibodies against DGs, SGs and hSSPN. DGC proteins were readily extracted from all muscles examined, as illustrated by the presence of these proteins in the soluble fraction (Fig. 6B). Completeness of digitonin solublization was confirmed by longer film exposures (data not shown). Examination of the insoluble pellet fractions demonstrates that the DGC was extracted to near completion for the non-Tg and non-phenotypic SSPN-Tg muscle (Fig. 6C). Only low levels of SG proteins and hSSPN were observed in the insoluble pellet fractions from the non-phenotypic SSPN-Tg muscle (Fig. 6C,D). However, high levels of α-, β- and γ-SG as well as hSSPN were detected in the detergent-insoluble pellet fraction from phenotypic SSPN-Tg muscle (Fig. 6C,D). In addition, higher order SSPN oligomers were present in insoluble fractions isolated from phenotypic SSPN-Tg muscle, but were not present to the same extent in non-phenotypic SSPN-Tgs (Fig. 6E). This homo-oligomerization may be responsible for SSPN-mediated clustering of the SG subcomplex into detergent-resistant protein aggregates within the plasma membrane. For all mice examined, α- and β-DG were extracted to near completion, indicating that SSPN does not cause aggregation of the DGs.

Destablization of α-DG in SSPN-Tg mice

Loss of the SG-SSPN subcomplex from the membrane causes destabilization of α-DG from the DGC, demonstrating that the SG-SSPN subcomplex helps to anchor α-DG to the sarcolemma (Duclos et al., 1998; Holt et al., 1998). In order to test for the stable attachment of α-DG to the DGC, we performed serial extraction experiments with increasing detergent stringencies. Skeletal muscle from SSPN-Tg and non-Tg mice was homogenized in 0.25% SDS and centrifuged to separate soluble (supernatant) from insoluble (pellet) proteins. Pellets from the 0.25% SDS extraction were resuspended in 0.5% SDS and subjected to another round of protein extraction, followed by three additional extractions in 1%, 2% and 3% SDS (Fig. 7A). Analysis of soluble fractions demonstrated that the majority of α-DG from non-Tg muscle is extracted only upon treatment with 1% SDS (Fig. 7B). Quantification of the α-DG levels extracted at 0.25%, 0.5% and 1% SDS is given for non-Tg, non-phenotypic SSPN-Tg and phenotypic SSPN-Tg mice in Fig. 7C. This SDS titration profile represents strong attachment of α-DG to the sarcolemma, as depicted in the schematic model (Fig. 7D). Lower concentrations of SDS (0.5%) efficiently extract α-DG from non-phenotypic SSPN-Tg muscle, suggesting that α-DG is less stably anchored to the DGC (Fig. 7B-D). The observation that α-DG is extracted with lower SDS stringency

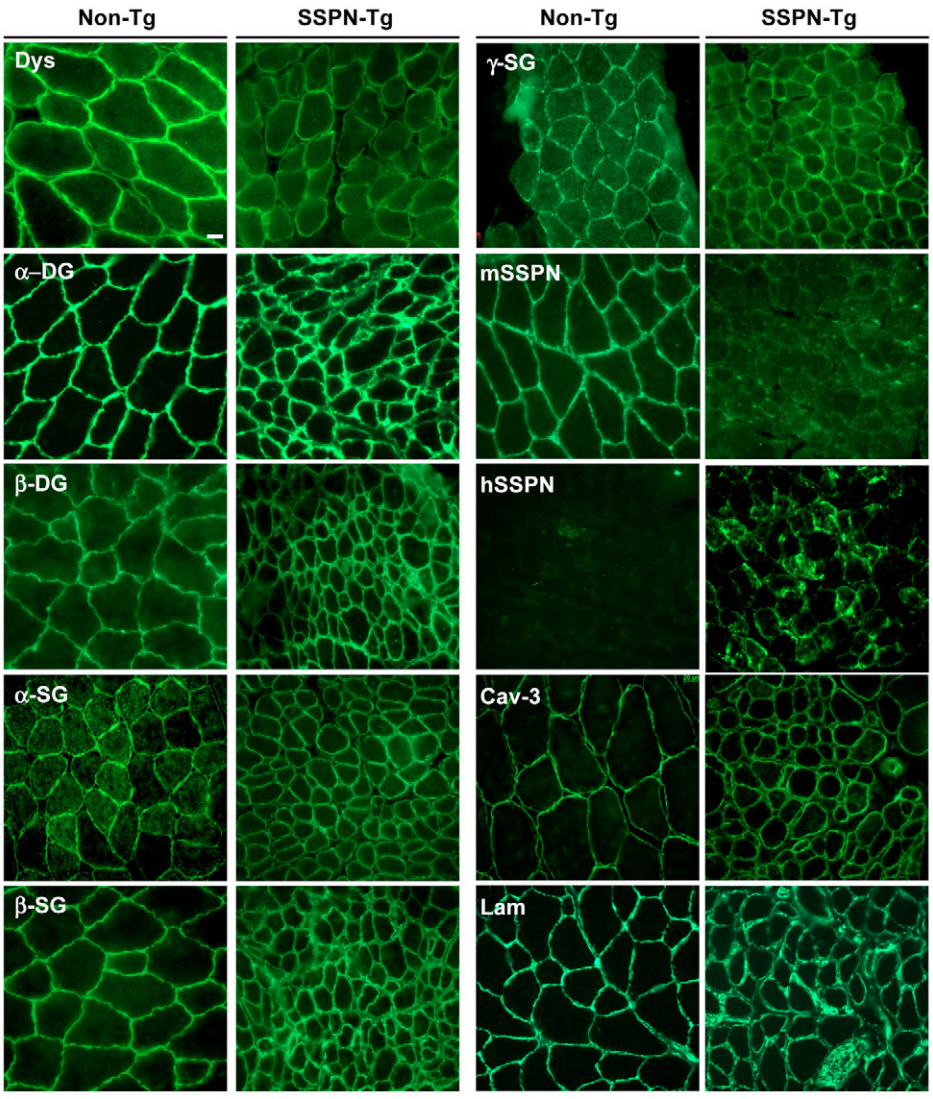

Fig. 5. SSPN expression does not perturb sarcolemma localization of the DGC. Immunohistochemical analysis of DGC and its associated proteins on transverse cryosections of quadriceps muscle from phenotypic SSPN-Tg and non-Tg mice. Sections were stained with antibodies to dystrophin (Dys), α- and β-DG, α-, β-, and γ-SG, caveolin-3 (Cav-3), and laminin (Lam). Staining of endogenous mouse SSPN (mSSPN) and exogenous human SSPN (hSSPN) is also shown. Bar, 20 μm.

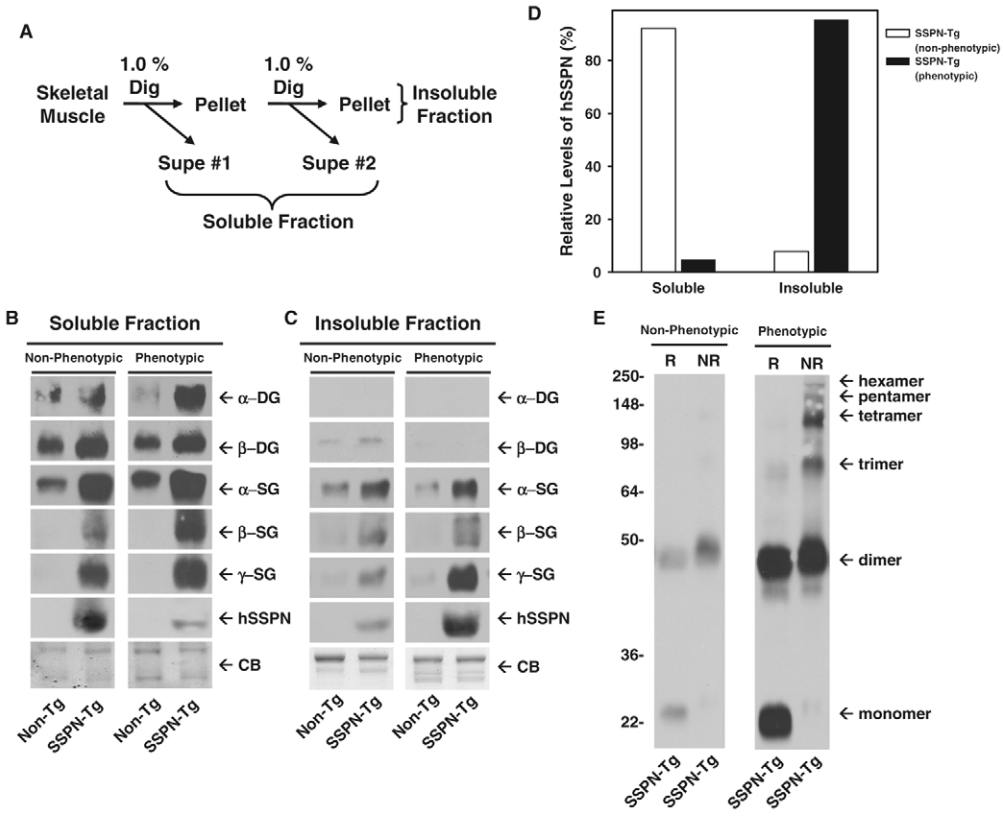

Fig. 6. SSPN induces aggregation of the SGs. (A) Schematic diagram to illustrate the experimental procedure. Following two 1% digitonin solubilizations (Supe #1 and Supe #2), insoluble protein aggregates were extracted using 3% SDS homogenization buffer. (B) Non-phenotypic and phenotypic SSPN-Tg (SSPN-Tg) muscle solubilized fractions contain more DGC proteins than non-Tg (Non-Tg) controls. Digitonin solubilized proteins (60 μg) were analyzed by 12% SDS-PAGE, transferred to nitrocellulose, and analyzed for components of the DGC by immunoblot analysis. Coomassie Blue (CB) stain was used to confirm equal loading of protein samples. (C) SDS solubilized proteins (60 μg) from non-Tg (Non-Tg) and SSPN-Tg (SSPN-Tg) were separated on 12% SDS-PAGE and transferred to nitrocellulose membranes. Representative data are shown from non-phenotypic (line 31.6) and phenotypic (line 31.7) SSPN-Tg mice. Nitrocellulose membranes were separately stained for α-DG and β-DG, α-SG, β-SG and γ-SG, as well as the SSPN transgene (hSSPN). Equal protein loading was confirmed by Coomassie Blue (CB) stain. (D) Quantification of transgene (hSSPN) solubilization. Percentage of solubilized protein was determined by relative densitometry. Relative levels of hSSPN in the soluble and insoluble fractions were analyzed for the phenotypic and non-phenotypic samples. Data is presented as percentages relative to the total level of transgene expression in the soluble and insoluble fractions combined. (E) SSPN homo-oligomerization in non-phenotypic and phenotypic insoluble fractions. SDS solubilized proteins (60 μg) from non-phenotypic and phenotypic SSPN-Tg muscle were analyzed by SDS-PAGE under reducing (R) or non-reducing (NR) conditions and transferred to nitrocellulose. Membranes were probed with antibodies recognizing transgene (hSSPN) expression. Higher-order SSPN oligomers were present only in extracts from phenotypic SSPN-Tg muscle.

conditions suggests that α-DG attachment to the DGC is slightly weakened or strained. Interestingly, α-DG from phenotypic SSPN-Tg muscle is readily extracted with even less (0.25%) SDS (Fig. 7B-D). These data support a model whereby overexpression of SSPN protein in phenotypic SSPN-Tg muscle weakens the interaction between α-DG and the DGC, possibly by increasing the spatial distance between the SG and DG subcomplexes. In addition, we analyzed the presence of laminin in each fraction and found that laminin was extracted under similar conditions as α-DG from non-Tg and non-phenotypic SSPN-Tg samples (Fig. 7B). Laminin and α-DG partitioned in the same fractions for non-Tg and non-phenotypic SSPN-Tg samples. Remarkably, laminin from phenotypic SSPN-Tg tissue was only extracted with high, denaturing concentrations of SDS (3%) (Fig. 7B). The presence of α-Dg and laminin in distinct fractions of the SDS titration indicates that these proteins are probably not forming proper protein-protein interactions. Furthermore, our data also suggest the large laminin accumulations, visualized by indirect immunofluorescence (Fig. 5), are indeed insoluble laminin aggregations. We propose that overexpression of SSPN causes hyper-clustering and aggregation of the SGs, which perturbs the ability of the SG-SSPN subcomplex to function as an anchorage for α-DG.

Perturbation of the extracellular matrix in SSPN-Tg muscle

Previous reports have shown that α-DG plays an important role in assembly of laminin-2 and perlecan within the extracellular matrix (Brown et al., 1999; Henry and Campbell, 1998; Henry et al., 2001; Kanagawa et al., 2005). We show that laminin extraction is only possible under denaturing

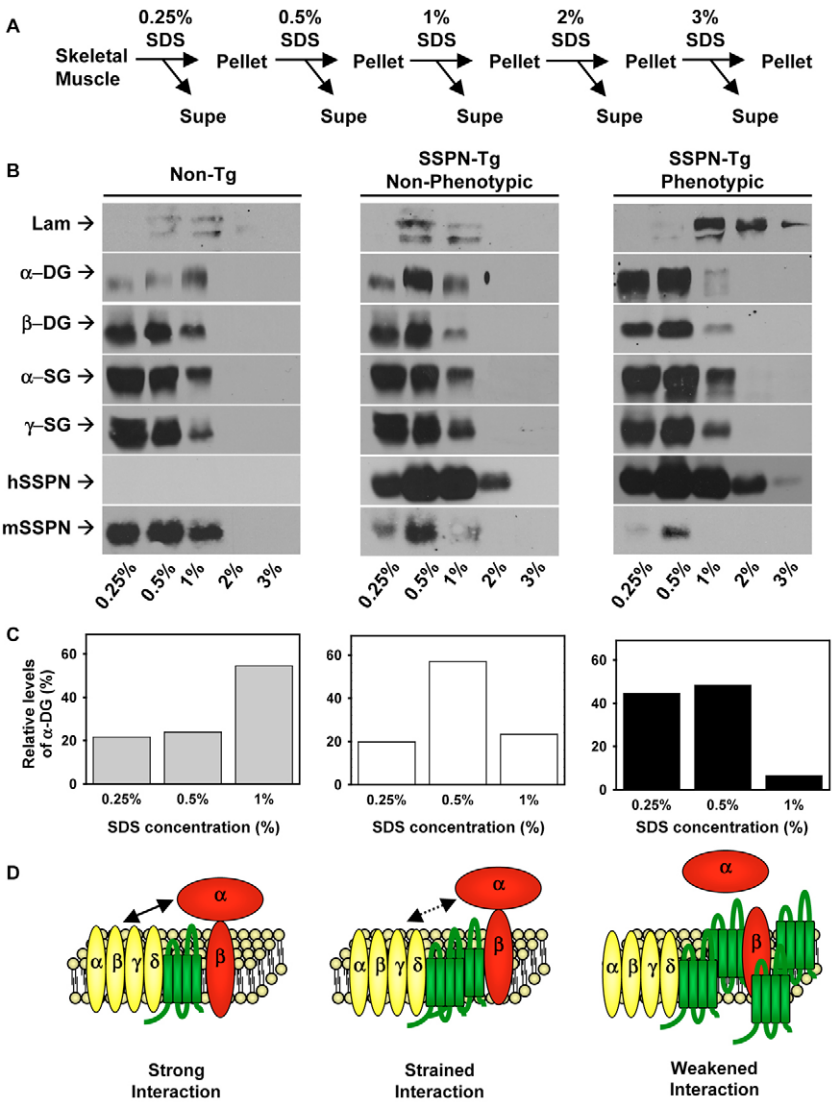

Fig. 7. α-DG is destabilized in phenotypic SSPN-Tg muscle. (A) Schematic diagram showing the steps in the SDS titration experiment. Skeletal muscle from non-Tg and SSPN-Tg mice was subjected to sequential extractions in lysis buffer with increasing SDS concentrations. Skeletal muscle was homogenized in 0.25% SDS and centrifuged to separate soluble (supe) from insoluble (pellet) proteins. The pellet was resuspended in a 0.5% SDS buffer for a second round of protein extraction. This process was repeated with 1%, 2% and 3% SDS. (B) Protein supernatants from each SDS titration were separated using SDS-polyacrylamide gels and transferred to nitrocellulose membranes. Immunoblots were stained with antibodies to laminin (Lam), α- and β-DG, α-, β-, and γ-SG, hSSPN, and mSSPN as indicated. 1% SDS was required to extract α-DG in non-Tg muscle, which represents a strong and stable attachment of α-DG to the DGC. In non-phenotypic SSPN-Tg muscle, α-DG is removed under lower stringency conditions (0.5% SDS), suggesting that α-DG is weakened by presence of SSPN overexpression. Finally, α-DG is readily extracted from phenotypic SSPN-Tg muscle with 0.25% SDS, supporting the hypothesis that SSPN destabilizes α-DG. (C) Densitometry of α-DG staining from immunoblots. Relative levels of α-DG found in the supernatant fraction after treatment with 0.25%, 0.50% and 1.0% was quantified for all muscle samples analyzed. (D) Schematic models illustrating α-DG attachment to the DGC in non-Tg, non-phenotypic SSPN-Tg, and phenotypic SSPN-Tg.

conditions for phenotypic SSPN-Tg muscle. Furthermore, the finding that α-DG is not stably attached to the sarcolemma in SSPN-Tg muscle raises the possibility that ligands of α-DG in the extracellular matrix may likewise have structural abnormalities. In order to investigate whether the SSPN-Tg phenotype correlates with disruption of the basement membrane, we analyzed collagen VI expression by indirect immunofluorescence staining of quadriceps muscles from SSPN-Tg and non-Tg mice. Collagen VI serves as a marker for structural integrity of the extracellular matrix. Although it is unclear what protein(s) is responsible for anchoring collagen VI to the basement membrane, collagen IV, perlecan and fibronectin basement membrane proteins have all been shown to interact with collagen VI in vitro (Kuo et al., 1997; Tillet et al., 1994). Genetic mutations in collagen VI are associated with Ullrich congenital MD and Bethlem myopathy (for a review, see Lampe and Bushby, 2005). In non-Tg muscle, collagen VI and perlecan are co-localized, as illustrated by the complete overlap of collagen VI and perlecan staining in merged images (Fig. 8A). Non-phenotypic SSPN-Tg muscle also displayed normal co-localization of perlecan and collagen VI (Fig. 8A). However, the overlap between perlecan and collagen VI was disrupted in phenotypic SSPN-Tg muscle (Fig. 8A). Similar uncoupling of perlecan and collagen VI occurs in muscle from patients with Ullrich congenital MD (Pan et al., 2003).

Because laminin is the primary ligand of α-DG in the extracellular matrix, identical co-localization experiments were performed with laminin and perlecan. Similar to the results reported for perlecan and collagen VI localization, perlecan and laminin co-localized in non-Tg and non-phenotypic SSPN-Tg muscle (Fig. 8B). Uncoupling of laminin and perlecan staining was only observed in the phenotypic SSPN-Tg muscle (Fig. 8B). Identical results were found for co-staining of non-Tg, non-phenotypic SSPN-Tg, and phenotypic SSPN-Tg muscle using laminin and collagen VI antibodies (data not shown). These findings provide additional support for the SDS titration experiments (Fig. 7B) and add strength to the conclusion that SSPN overexpression disrupts the linkage between α-DG and laminin. The disorganization of collagen VI, perlecan, and laminin in the phenotypic SSPN-Tg muscle is strongly indicative of gross structural defects in the extracellular matrix.

As an additional method to examine the structural integrity

of the extracellular matrix and the sarcolemma, electron microscopy was performed on non-Tg and phenotypic SSPN-Tg muscle. Electron micrographs of EDL muscles reveal that SSPN-Tg muscle possesses normal sarcomere structures (Fig. 9A). Defects in the sarcolemma of SSPN-Tg muscle were not observed, supporting data from the Evans Blue dye and creatine kinase assays (Fig. 3). However, the distances between sarcolemma of adjacent myofibers appeared to be greater in the SSPN-Tg muscle compared with non-Tg controls (white arrows, Fig. 9A,B). Photomicrographs of the sarcolemma taken at higher magnification show that the extracellular matrix in SSPN-Tg muscle is characterized by randomly placed, unorganized dense clumps (black arrows, Fig. 9B). By contrast, the extracellular matrix from non-Tg muscle appeared to be a tight, linear structure that was closely aligned in a parallel fashion with the sarcolemma (Fig. 9B). The disorganization of the basement membrane in SSPN-Tg muscle may account for the larger spacing between neighboring myofibers. Perturbation of the extracellular matrix represents a likely pathological mechanism for the severe and lethal dystrophic phenotype observed in the SSPN-Tg mice, as proposed in our model (Fig. 10).

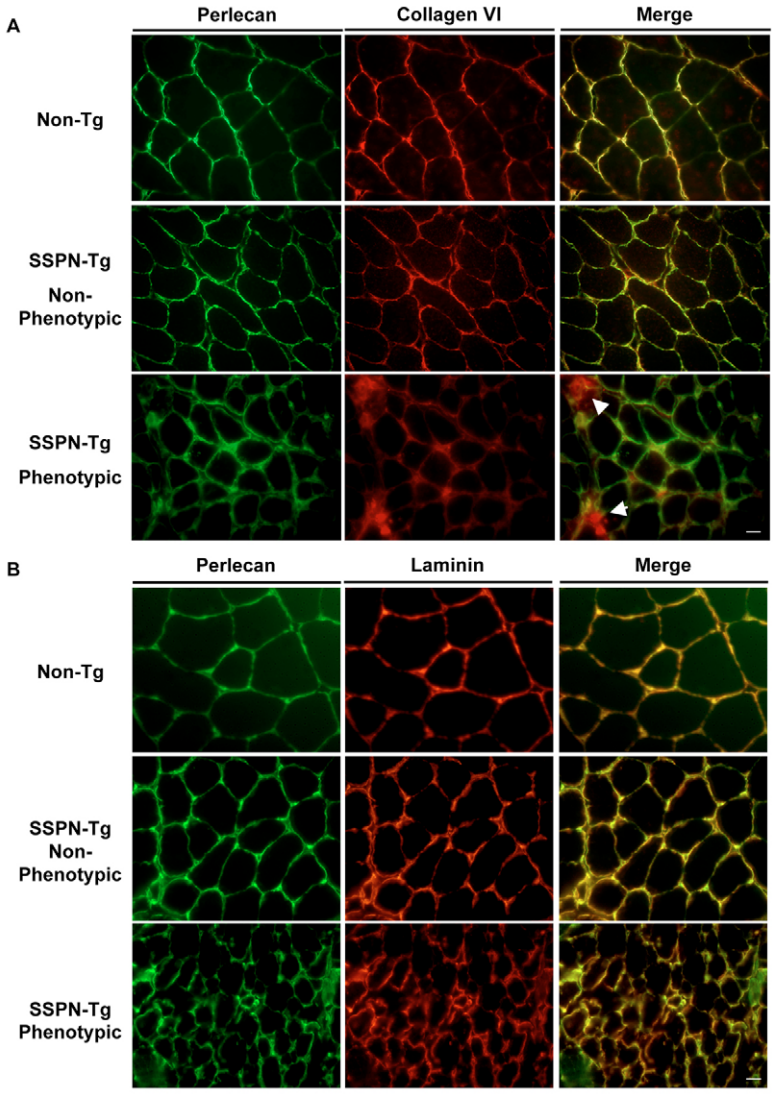

Fig. 8. Disruption of basement membrane organization in SSPN-Tg muscle. Immunostaining of transverse quadriceps sections from non-Tg, non-phenotypic SSPN-Tg (line 31.6), and phenotypic SSPN-Tg (line 37.5) mice. Sections were co-stained with (A) monoclonal antibodies against perlecan (green) and collagen VI (red) or (B) antibodies against perlecan (green) and laminin (red). Merged images of green and red fluorescence are shown in the far right panel. In normal muscle (non-Tg and non-phenotypic SSPN-Tg), perlecan completely co-localizes with collagen VI (A) or laminin (B) at the basement membrane. In muscle from the phenotypic SSPN-Tg mice, collagen VI is present in the basement membrane but appears patchy and reduced in intensity relative to the perlecan and laminin. Collagen VI staining is increased in the interstitial and perivascular space (arrows). Collagen VI and laminin are not co-localized with perlecan in phenotypic SSPN-Tg mice, as demonstrated in merged images. Bar, 50 μm.

Discussion

Primary mutations in many components of the DGC cause numerous forms of clinically distinct muscular dystrophies. Mutations in the dystrophin gene are responsible for Duchenne MD (Hoffman et al., 1987). Genetic defects in α-, β-, γ-, or δ-SG cause autosomal-recessive limb-girdle MD (for a review, see Durbeej and Campbell, 2002). In most cases, loss of one SG results in absence of the entire SG-SSPN subcomplex from the sarcolemma, which suggests that all members of the DGC complex are required for stability of this transmembrane protein complex (for a review, see Durbeej and Campbell, 2002). Although the function of the complex is not entirely understood, both mechanical and signaling functions have been ascribed to the DGC. It has been proposed that the physical linkage between the actin cytoskeleton and the extracellular matrix (via the DGC) provides protection to the sarcolemma during muscle contractions (Ervasti and Campbell, 1993; Lynch et al., 2000). Indeed, sarcolemma fragility is one of the hallmark characteristics of muscular dystrophies associated with loss of the DGC in skeletal muscle (Lynch et al., 2000; Petrof et al., 1993; Weller et al., 1990). Recent studies from Chamberlain's group provide additional support for the important mechanical role of the DGC in muscle (Judge et al., 2006). Therefore, identifying the structural elements that are necessary for proper DGC complex stability represents an important step toward designing smart therapeutics aimed at stabilizing the DGC in the sarcolemma.

Structural analysis of SSPN suggests that it is perfectly poised to play an important role in determining the stability of the DGC (Crosbie et al., 1997). SSPN possesses four transmembrane domains and shares some homology to the tetraspanin superfamily of proteins (Crosbie et al., 1997). As a group, the tetraspanins are thought to organize transmembrane protein complexes within the membrane bilayer (for a review, see Hemler, 2003; Levy and Shoham, 2005). Data presented here suggests that SSPN forms higher-order oligomeric complexes that may serve to promote protein-protein interactions within the DGC (Fig. 6E). Although we

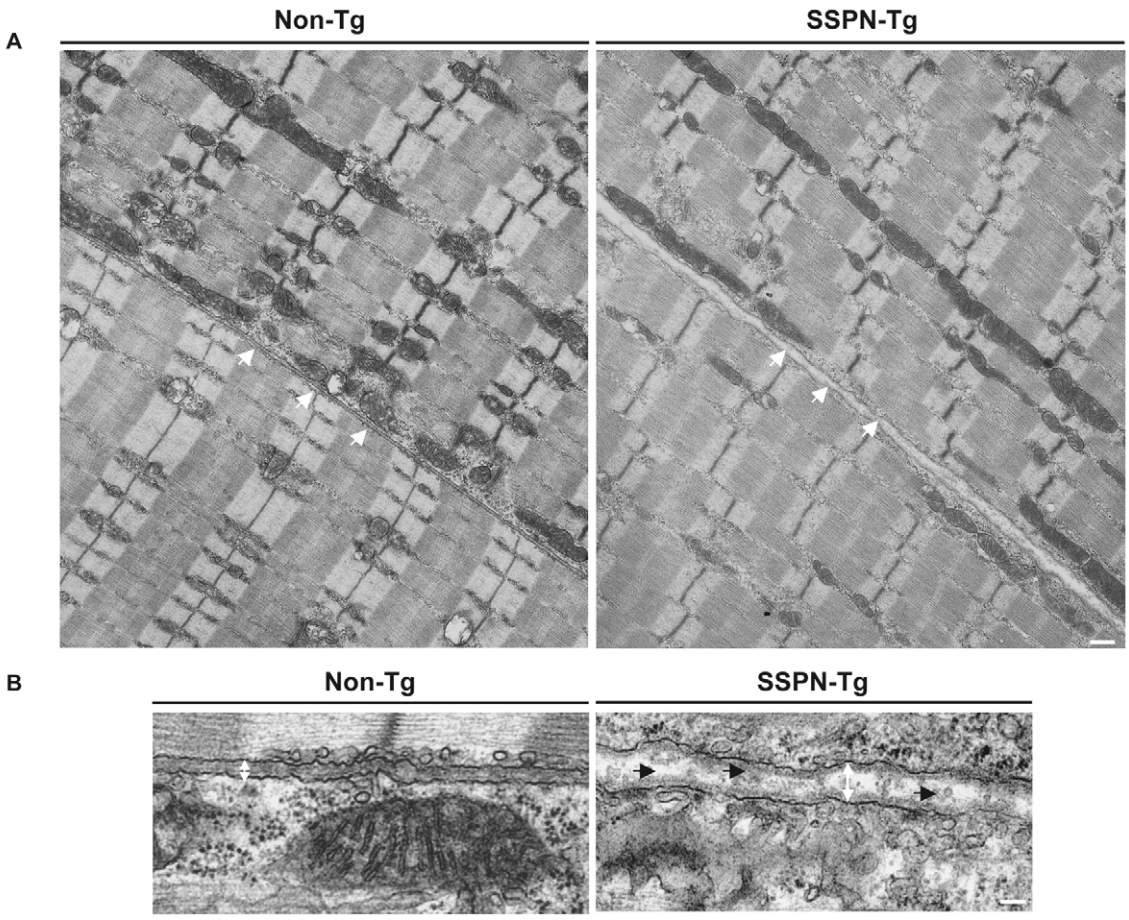

Fig. 9. Electron micrographs reveal structural defects in basement membrane. (A) Electron micrographs of longitudinal sections of EDL muscles isolated from phenotypic SSPN-Tg and non-Tg mice. Two neighboring muscle fibers are shown in each field. The sarcolemma is denoted by arrows. Bar, 1 μm. (B) Electron micrographs were taken at higher magnifications to visualize the basement membrane. The distance between adjacent sarcolemmas is greater in the SSPN-Tg muscle than in the non-Tg muscle (white arrows). The extracellular matrix is visualized as a tight linear structure between two neighboring sarcolemmas in the non-Tg tissue. However, the extracellular matrix is randomly placed in dense, disorganized clumps in the phenotypic SSPN-Tg muscle (black arrows). Bar, 200 nm.

propose an important role for SSPN within the DGC, data from the SSPN-deficient mice (Lebakken et al., 2000) has not provided much insight into SSPN's function. SSPN-null mice exhibit wild-type levels of DGC protein expression and possess normal force and power generation capabilities (Lebakken et al., 2000). It is feasible that SSPN is replaced by a functionally similar tetraspanin during muscle development, which does not clarify the interpretation of SSPN's role in muscle physiology.

As an alternative approach to investigating the function of SSPN within the DGC, we engineered SSPN-Tg mice that overexpress SSPN protein in skeletal muscle. We have characterized five lines of SSPN-Tg mice with varying levels of SSPN. Two transgenic lines with high SSPN protein expression displayed gross physical abnormalities consisting of kyphosis, reduced body mass and mobility defects. These lines of mice died by 10-weeks of age and were not successfully maintained because of the lethal nature of the SSPN overexpression. Muscle from the high expressing SSPN-Tg mice was characterized by elevated central nucleation and variation in fiber size. Two lines with low SSPN protein expression were indistinguishable from non-Tg controls and did not exhibit muscle histopathology. None of the SSPN-Tg mice displayed Evans Blue dye accumulation in myofibers or elevated serum creatine kinase levels, suggesting that sarcolemma integrity was not compromised by SSPN protein overexpression. Thus, the severe phenotype of the SSPN-Tg mice could not be explained by membrane instability.

Protein interactions within the DGC can be categorized as occurring either within or across the plane of the membrane. The SG-SSPN subcomplex and β-DG are transmembrane proteins that interact laterally with one another in the sarcolemma. Dystrophin and the DGs provide a structural linkage across the sarcolemma to connect the extracellular matrix with intracellular F-actin (for a review, see Durbeej and Campbell, 2002). We found that SSPN perturbed both types of interactions in SSPN-Tg muscle. We propose that SSPN-mediated aggregation of the SGs causes destabilization of α-DG attachment to the sarcolemma, which, in turn, leads to perturbation of basement membrane formation (Fig. 10). Taken together, our data support a model whereby SSPN overexpression disrupts protein interactions within and across the membrane bilayer (Fig. 10). SSPN expression caused clustering of the SGs into detergent insoluble aggregates, which were never observed in wild-type mice. Non-phenotypic

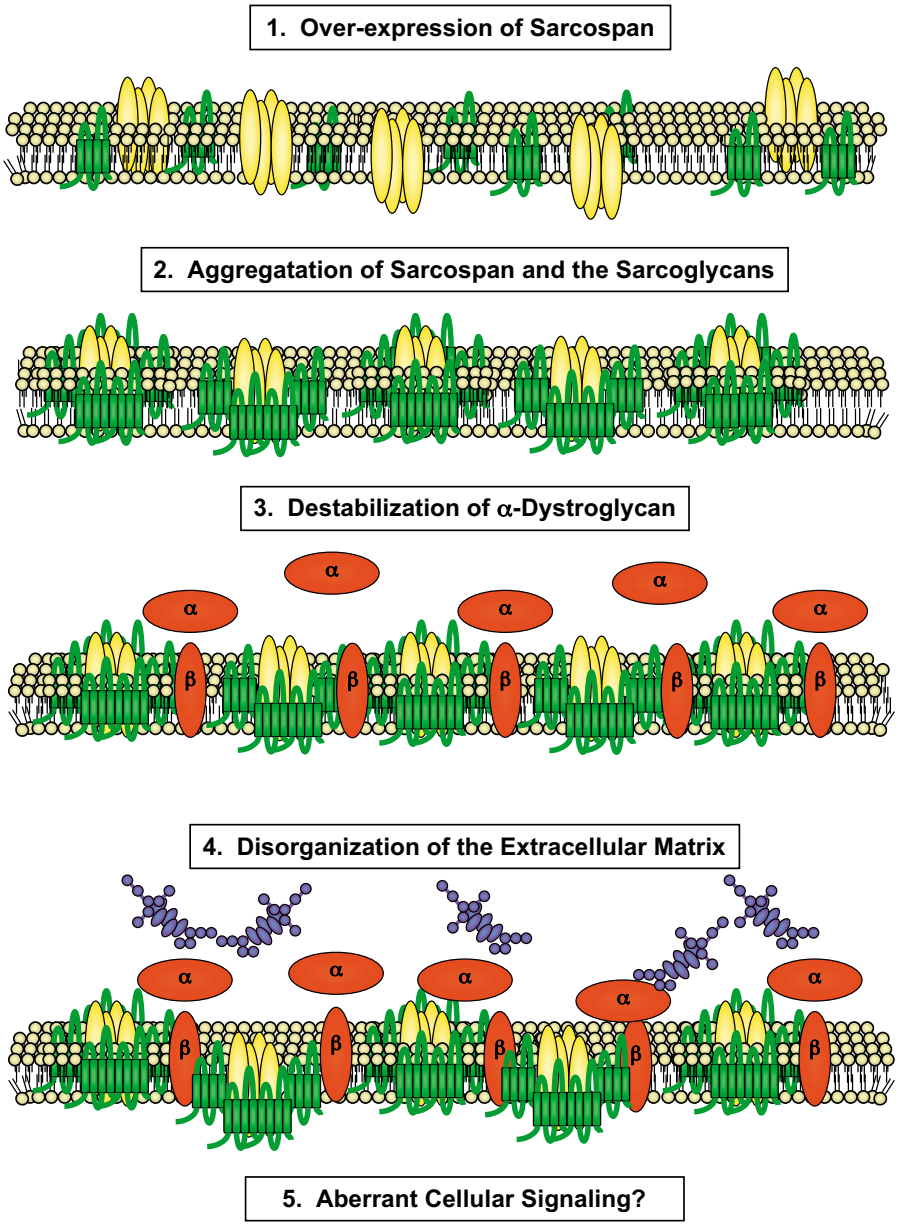

Fig. 10. Schematic diagram showing a pathogenetic mechanism for SSPN-mediated disruption of the DGC. The data in the current report support a model of SSPN-induced dysfunction of the DGC. We propose that SSPN (green) overexpression at the sarcolemma (1) causes clustering of the SGs (yellow) into insoluble aggregates (2). Perturbation of the SG-SSPN subcomplex within the DGC impairs its ability to properly anchor α-DG (red) at the sarcolemma (3). The destabilization of α-DG attachment to the sarcolemma leads to perturbation of basement membrane (blue) assembly (4). It is feasible that disruption of the basement membrane leads to aberrant cellular signaling (5), which may be responsible for the increased levels of apoptosis in phenotypic SSPN-Tg mice. By this pathogenetic mechanism, SSPN disrupts protein interactions within and across the membrane bilayer leading to a severe phenotype that is reminiscent of congenital MD.

SSPN-Tg mice displayed only low levels of SG protein aggregation. We provide data to suggest that SSPN overexpression drives formation of SSPN hyper-oligomers within the sarcolemma. We propose that such abnormal SSPN structures disrupt proper SG protein interactions by trapping the SGs into insoluble protein aggregates.

One function of the SG-SSPN subcomplex is to stabilize α-DG at the sarcolemma (Holt et al., 1998). By examining extraction of α-DG with SDS, we show that disruption of proper SG-SSPN protein interactions within the sarcolemma of SSPN-Tg muscle results in destabilization of α-DG. The role of α-DG in organization of the extracellular matrix has been well-established (Brown et al., 1999; Henry and Campbell, 1998; Henry et al., 2001; Kanagawa et al., 2005). We now show that SSPN overexpression disrupts formation of the extracellular matrix, as revealed by uncoupling of perlecan, laminin and collagen VI co-localization and as seen by electron microscopy. Laminins represent one of the major components of the extracellular matrix and mutations in the *LAMA2* gene, which encodes laminin-α2 chain, cause congenital MD (Allamand et al., 1997; Helbling-Leclerc et al., 1995; Miyagoe-Suzuki et al., 2000). Although the DGC is normally expressed in mouse models with defects in laminin (*dy*/*dy*, dy^{w}/dy^{w}, dy^{3k}/dy^{3k}, dy^{Pas}/dy^{Pas}, dy^{2j}/dy^{2j}; *dy* = *Lama2*), the linkage between the extracellular matrix and the cytoskeleton is disrupted (Besse et al., 2003; Guo et al., 2003; Kuang et al., 1998; Miyagoe et al., 1997; Sunada et al., 1994; Xu et al., 1994). We provide data to demonstrate that the extracellular matrix, including laminin, exhibits abnormal structure in phenotypic SSPN-Tg muscle. Taken together, our data support a necessary role for SSPN in organizing proteins within the DGC and in assembly of the extracellular matrix.

Relatively low levels of SSPN protein expression (10-fold over endogenous levels) resulted in severe toxicity. This is

intriguing since high levels of transgenic dystrophin or utrophin protein in skeletal muscle increase expression of the other DGC components *without* toxicity (Rafael et al., 1996; Rafael et al., 1994; Rafael et al., 1998). SSPN protein expression was not stoichiometric with respect to the other DGC components. This observation suggests that the molar ratio of SSPN to the other DGC components is important and that regulating the levels of SSPN within the myofiber is critical for normal muscle function. Such findings support the hypothesis that SSPN regulates protein interactions within the DGC and that increasing the stoichiometry of SSPN relative to the DGC is highly toxic. Taken together, our data are the first to suggest that SSPN may indeed play an important role in muscle physiology. Previous searches for patients with genetic mutations in the SSPN gene have focused on sarcoglycan-deficient muscular dystrophies. Despite extensive efforts, SSPN mutations have not been identified in cases of AR-LGMD (Crosbie et al., 2000). In light of the apparent role of SSPN-mediated stability of α-DG and the extracellular matrix, the current report provides evidence to suggest that SSPN may also be involved in congenital muscular dystrophies.

Materials and Methods

Mice

Wild-type (C57BL/6) and *mdx* (*Dmd*; Mouse Genome Informatics) mice were obtained from Jackson Laboratories (Bar Harbor, ME, USA) and maintained at the Life Sciences Vivarium.

Generation of SSPN-Tg mice

Human SSPN ORF (AF016028; Fig. 1A) was subcloned into the pBSX-HSAvpA expression vector (Crawford et al., 2000), which was kindly provided by Dr Jeffrey S. Chamberlain (University of Washington School of Medicine, Seattle, WA, USA). This previously described plasmid contains a SV40 VP1 intron located downstream of the human skeletal α-actin promoter (Crawford et al., 2000). Sarcospan transgenic mice (SSPN-Tg) were generated at the University of California Irvine, Transgenic Mouse Facility by microinjection of linearized, purified plasmid into F_2 hybrid zygotes from C57BL/6×BALB/c parents, as described previously (Miller et al., 2006; Spencer et al., 2002; Spencer and Mellgren, 2002; Taveau et al., 2002; Tidball and Spencer, 2002). Thirty-one founder (F_0) mice were generated and these F_0 mice were crossed with C57BL/6. SSPN-Tg mice were identified by PCR analysis as previously described (Spencer et al., 2002; Spencer and Mellgren, 2002; Taveau et al., 2002; Tidball and Spencer, 2002). Analysis of phenotypic SSPN-Tg animals (lines 31.7 and 37.5) could only be performed with N_1 generation mice because of the lethality of SSPN transgene expression. All experiments were performed with age-matched, non-Tg littermates. Procedures involving live mice were approved by the University of California Institutional Animal Care and Use Committee.

Sarcospan antibodies

Antibodies to mouse SSPN (Rabbit 3) and to human SSPN (Rabbit 15) were described previously (Miller et al., 2006). To generate antibodies that cross-react with both human and mouse SSPN, a New Zealand white rabbit (Irish Farms, Norco, CA, USA) was injected with 500 μg of recombinant SSPN fusion protein (Rabbit 18). The SSPN fusion protein was engineered by fusing maltose binding protein (MBP) with the C-terminal region of mouse SSPN (SSPN aa 186-216, GenBank accession number U02487).

Histology

In order to assess muscle pathology and central nucleation of muscle fibers, transverse sections from quadriceps, tibialis anterior, soleus and diaphragm muscles (8 μm) were stained with Hematoxylin and Eosin as described previously (Peter and Crosbie, 2006). The percentage of centrally nucleated fibers was assessed for quadriceps muscle isolated from two non-Tg and four SSPN-Tg mice representing the two phenotypic transgenic lines. Data are presented as the mean percentage (± standard error) of total fibers counted for both non-Tg and SSPN-Tg mice. Statistical analysis was performed using the *t*-test function in SigmaPlot® (Systat Software, Inc., Point Richmond, CA, USA). Photomicrographs were obtained as described below.

TdT-dUTP labeling

To address whether cells were actively undergoing apoptosis, transverse tibialis anterior sections (8 μm) were used for TdT-mediated dUTP end-labeling analysis as previously described (Tidball et al., 1995). An Avidin/Biotin Blocking kit (Vector laboratories, Burlingame, CA, USA) was used according to the manufacturer's instructions to decrease background reactivity to the biotin conjugated dUTP. Sections were visualized as described below.

Immunofluorescence

For single labeling experiments, quadriceps muscle cryosections (8 μm) were prepared utilizing a Leica CM 3050S cryostat (Leica Microsystems, Bannockburn, IL, USA). Sections were stored on positively charged glass slides (VWR, West Chester, PA, USA) at –80°C for future analysis. Before analysis, sections were left at RT for 15 minutes. After blocking in 3% BSA diluted in PBS, sections were incubated with antibodies to dystrophin (1:10; University of Iowa, Hybridoma Facility), α-DG (1:100; Upstate Signaling, Lake Placid, NY, USA, VIA4-1) β-DG (1:50; Vector Laboratories, VP-B205), α-, β- and γ-SG (1:100, VP-A105; 1:200, VP-B206; and 1:50, VP-G803 respectively; Vector Laboratories), caveolin-3 (1:500; BD Biosciences, San Diego, CA, 610420) and laminin (1:40; Sigma Chemical Co., St Louis, MO, USA, L9393). Antibodies to mouse SSPN (Rabbit 3, neat) and human SSPN (Rabbit 15; 1:25) have been described previously (Miller et al., 2006). Sections were fixed with ice-cold acetone for 10 minutes, at RT, before antibodies to collagen-3 and -4 (1:50; Southern Biotech, Birmingham, AL, USA, 1330-1 and 1340-1; respectively) were utilized. For co-localization experiments, sections were briefly fixed with methanol at RT for 20 seconds and washed before the addition of antibodies to collagen VI (1:2500; Chemicon International, MAB3303), laminin (1:1000; Sigma Chemical Co., L9393) and perlecan (1:1000; Chemicon International, MAB1948). All sections were visualized using an Axioplan 2 fluorescence microscope (Carl Zeiss Inc, Thornwood, NY, USA) and digitized images were captured under Axiovision 3.0 software (Carl Zeiss Inc.).

Evans Blue tracer assay

Evans Blue dye (EBD) was diluted in PBS (10 mM phosphate buffer, 150 mM NaCl, pH 7.4) to a final concentration of 10 mg/ml and was sterilized by filtration using a 0.2 μm filter. Peritoneal cavity injection of 50 μl of EBD per 10 g of body weight was performed on 8-week old non-TG and SSPN-TG littermates. For positive control, age-matched *mdx* mice were also injected. 16 hours post-injection, muscles were excised and frozen in liquid nitrogen-cooled isopentane. Transverse cryosections (8 μm) of quadriceps muscles were incubated with ice-cold acetone, washed 3× 10 minutes with PBS, and mounted with Vectashield (Vector laboratories). EBD-positive muscle fibers were observed using a fluorescence microscope, as previously described (Matsuda et al., 1995).

Serum creatine kinase assay

Blood was collected from the retro-orbital sinus of 4-week old SSPN-Tg, non-Tg and *mdx* mice. Total creatine kinase (CK) levels in serum were measured with a Beckman Coulter UV spectrometer (Fullerton, CA, USA) using a creatine kinase reagent (CK-NAC; Teco diagnostics, Anaheim, CA, USA) according to the manufacturer's instructions. Serum taken from *mdx* mice was diluted 1:20 before assay was completed to ensure measurements were taken in the linear range of the assay.

Preparation of total protein lysates from skeletal muscle

Skeletal muscle isolated from either non-TG or SSPN-TG mice was pulverized in liquid nitrogen using a mortar and pestle. The powdered muscle was homogenized in 10 volumes of cold lysis buffer (3% SDS, 0.115 M sucrose, 0.066 M Tris-HCl, pH 7.4). Lysis buffer was chilled immediately before use to avoid the possibility of SDS precipitation. Before homogenization, protease inhibitors (0.6 μg/ml pepstatin A, 0.5 μg/ml aprotinin, 0.5 μg/ml leupeptin, 0.75 mM benzamidine, and 0.1 mM PMSF) were added to lysis buffer. The muscle homogenate was rotated at 4°C for 1 hour and clarified by centrifuging at 15,000 ***g*** for 15 minutes. Following centrifugation, supernatant was removed to pre-chilled tubes. Protein concentrations were determined using the DC Protein Assay® (Bio-Rad, Hercules, CA, USA). Equal concentrations of protein samples (60 μg) were resolved by 8% or 12% SDS-PAGE and transferred to nitrocellulose membranes (Millipore Corp., Billerica, MA, USA) for subsequent immunoblotting. Immunoblotting was performed on nitrocellulose transfers using the following antibodies: dystrophin (University of Iowa, Hybridoma Facility, MANDYS1; 1:10), laminin (Sigma, L9393; 1:5000), α-DG (Upstate Cell Signaling, VIA4-1; 1:1000), β-DG (University of Iowa, Hybridoma Facility, MANDAG2; 1:250), α-SG (Vector Laboratories, VP-A105; 1:100), β-SG (Vector Laboratories, VP-B206; 1:100), γ-SG (Vector Laboratories, VP-G803; 1:100) and caveolin-3 (BD Biosciences; 1:2500). To compare the level of endogenous (mSSPN) and exogenous (hSSPN) SSPN expression, a membrane was probed with polyclonal antibodies that recognize both proteins (crude serum, Rabbit 18; 1:500). Horseradish peroxidase-conjugated anti-rabbit IgG and anti-mouse IgG (Amersham Pharmacia Biotech, Piscataway, NJ, USA) secondary antibodies were used at a 1:3000 dilution. Enhanced chemiluminescence with SuperSignal West Pico Chemiluminescent Substrate (Pierce, Rockford, IL, USA) was used to develop all immunoblots.

Purification of the dystrophin-glycoprotein complex

The DGC was extracted from skeletal muscle tissue using 1% digitonin (Biosynth, Naperville, IL, USA) from non-transgenic (Non-Tg), non-phenotypic SSPN-transgenic (SSPN-Tg line 31.6) and phenotypic SSPN-transgenic (SSPN-Tg line 31.7). Following solubilization, 60 μg of muscle lysates were analyzed by 12% SDS-PAGE, transferred to nitrocellulose, and probed with antibodies to the DGC and the transgene as described above. To enrich for α-DG, equal protein concentrations of clarified lysates were applied to succinylated wheat germ agglutinin (sWGA) columns (Vector Laboratories Inc), as described previously (Campbell and Kahl, 1989). Following 0.1% digitonin washes, bound proteins were subsequently eluted from the column with *N*-acetyl glucosamine. 60 μl of each elution was electrophoresed by 10% SDS-PAGE and transferred to nitrocellulose.

After the soluble fraction was removed, the pellets, consisting of insoluble proteins, were incubated with lysis buffer (3% SDS, 0.115 M sucrose, 0.066 M Tris-HCl, pH 7.4) containing protease inhibitors (0.6 μg/ml pepstatin A, 0.5 μg/ml aprotinin, 0.5 μg/ml leupeptin, 0.75 mM benzamidine, and 0.1 mM PMSF). After centrifugation, 60 μg of each insoluble fraction was analyzed by 12% SDS-PAGE, transferred to nitrocellulose, and analyzed for components of the DGC and transgene expression as described above. Horseradish peroxidase-conjugated anti-mouse IgG and anti-rabbit IgG (Amersham Pharmacia Biotech) secondary antibodies were used at a 1:3000 dilution. Detection was completed as described above.

SDS titration experiments

Total skeletal muscle tissue from non-Tg, non-phenotypic SSPN-Tg and phenotypic SSPN-Tg was snap frozen in liquid nitrogen and stored at –80°C for future use. Tissue was subsequently homogenized in 10 volumes of lysis buffer (0.115 M sucrose, 0.066 M Tris-HCl, pH 7.4) containing 0.25% SDS and protease inhibitors (0.6 μg/ml pepstatin A, 0.5 μg/ml aprotinin, 0.5 μg/ml leupeptin, 0.75 mM benzamidine and 0.1 mM PMSF). The homogenate was rotated for 1 hour, at 4°C, then clarified by centrifugation at 15,000 ***g*** for 15 minutes. The supernatant was removed and stored on ice. The pellet was resuspended in lysis buffer containing 0.5% SDS and rotated for 1 hour, at 4°C, clarified by centrifugation at 15,000 ***g*** for 15 minutes, and the supernatant was removed. The pellet was subsequently homogenized in lysis buffers containing 1%, 2% and 3% SDS as described above. 40 μl of each supernatant was analyzed by SDS-PAGE on 12% isocratic gels and transferred to nitrocellulose membranes. Membranes were probed with antibodies to DGC components as described above. Blots were developed as described above. AlphaImager® (Alpha Innotech, San Leandro, CA, USA) was employed to quantify the density of protein bands on immunoblots developed within the linear range of the autoradiography film. Data are presented as percentages of total protein level in the first three SDS extractions (0.25-1%).

Electron microscopy

The extensor digitorum longus (EDL) muscle from 5-week old SSPN-Tg and non-Tg littermates was fixed in 1.4% glutaraldehyde in 0.2 M cacodylate buffer, pH 7.2, for 30 minutes on ice, followed by buffer rinse, and fixation for 30 minutes in 1% osmium tetroxide. Samples were dehydrated in a graded series of ethanol and embedded in epoxy resin before thin sectioning and visualizing on a JEOL 100CX microscope with an integrated camera.

We thank Jeffrey S. Chamberlain (University of Washington, Seattle) for transgenic expression plasmids and Birgitta Sjostrand (UCLA) for assistance with electron microscopy. We kindly thank Erica Espinoza, Suhn Kyong Rhie, and Catherine L. Chu (UCLA) for their technical assistance. We are indebted to Melissa J. Spencer (UCLA) for guidance with transgene construction. We thank James G. Tidball (UCLA) for his assistance with electron microscopy tissue fixation. A.K.P. was supported by a Molecular, Cellular and Integrative Physiology pre-doctoral training fellowship (NIH: T32GM65823), the Edith Hyde Fellowship, and the Ursula Mandel Fellowship. This work was supported by the Muscular Dystrophy Association (MDA3704 to G.M.) and the NIH (AR48179-01 to R.H.C.).

References

Adams, M. E., Butler, M. H., Dwyer, T. M., Peters, M. F., Murnane, A. A. and Froehner, S. C. (1993). Two forms of mouse syntrophin, a 58 kd dystrophin-associated protein, differ in primary structure and tissue distribution. *Neuron* **11**, 531-540.

Allamand, V., Sunada, Y., Salih, M. A., Straub, V., Ozo, C. O., Al-Turaiki, M. H., Akbar, M., Kolo, T., Colognato, H., Zhang, X. et al. (1997). Mild congenital muscular dystrophy in two patients with an internally deleted laminin alpha2-chain. *Hum. Mol. Genet.* **6**, 747-752.

Besse, S., Allamand, V., Vilquin, J. T., Li, Z., Poirier, C., Vignier, N., Hori, H., Guenet, J. L. and Guicheney, P. (2003). Spontaneous muscular dystrophy caused by a retrotransposal insertion in the mouse laminin alpha2 chain gene. *Neuromuscul. Disord.* **13**, 216-222.

Bonnemann, C. G., Modi, R., Noguchi, S., Mizuno, Y., Yoshida, M., Gussoni, E., McNally, E. M., Duggan, D. J., Angelini, C. and Hoffman, E. P. (1995). Beta-sarcoglycan (A3b) mutations cause autosomal recessive muscular dystrophy with loss of the sarcoglycan complex. [published erratum appears in *Nat. Genet.* 1996 Jan;12(1):110]. *Nat. Genet.* **11**, 266-273.

Brown, S. C., Fassati, A., Popplewell, L., Page, A. M., Henry, M. D., Campbell, K. P. and Dickson, G. (1999). Dystrophic phenotype induced in vitro by antibody blockade of muscle alpha-dystroglycan-laminin interaction. *J. Cell Sci.* **112**, 209-216.

Campbell, K. P. and Kahl, S. D. (1989). Association of dystrophin and an integral membrane glycoprotein. *Nature* **338**, 259-262.

Coral-Vazquez, R., Cohn, R. D., Moore, S. A., Hill, J. A., Weiss, R. M., Davisson, R. L., Straub, V., Barresi, R., Bansal, D., Hrstka, R. F. et al. (1999). Disruption of the sarcoglycan-sarcospan complex in vascular smooth muscle: a novel mechanism for cardiomyopathy and muscular dystrophy. *Cell* **98**, 465-474.

Crawford, G. E., Faulkner, J. A., Crosbie, R. H., Campbell, K. P., Froehner, S. C. and Chamberlain, J. S. (2000). Assembly of the dystrophin-associated protein complex does not require the dystrophin COOH-terminal domain. *J. Cell Biol.* **150**, 1399-1410.

Crosbie, R. H., Heighway, J., Venzke, D. P., Lee, J. C. and Campbell, K. P. (1997). Sarcospan: the 25kDa transmembrane component of the dystrophin-glycoprotein complex. *J. Biol. Chem.* **272**, 31221-31224.

Crosbie, R. H., Yamada, H., Venzke, D. P., Lisanti, M. P. and Campbell, K. P. (1998). Caveolin-3 is not an integral component of the dystrophin-glycoprotein complex. *FEBS Lett.* **427**, 279-282.

Crosbie, R. H., Lebakken, C. S., Holt, K. H., Venzke, D. P., Straub, V., Lee, J. C., Grady, R. M., Chamberlain, J. S., Sanes, J. R. and Campbell, K. P. (1999). Membrane targeting and stabilization of sarcospan is mediated by the sarcoglycan subcomplex. *J. Cell Biol.* **145**, 153-165.

Crosbie, R. H., Lim, L. E., Moore, S. A., Hirano, M., Hays, A. P., Maybaum, S. W., Collin, H., Dovico, S. A., Stolle, C. A., Fardeau, M. et al. (2000). Molecular and genetic characterization of sarcospan: insights into sarcoglycan-sarcospan interactions. *Hum. Mol. Genet.* **9**, 2019-2027.

Dalkilic, I. and Kunkel, L. M. (2003). Muscular dystrophies: genes to pathogenesis. *Curr. Opin. Genet. Dev.* **13**, 231-238.

Duclos, F., Straub, V., Moore, S. A., Venzke, D. P., Hrstka, R. F., Crosbie, R. H., Durbeej, M., Lebakken, C. S., Ettinger, A. J., van der Meulen, J. et al. (1998). Progressive muscular dystrophy in alpha-sarcoglycan-deficient mice. *J. Cell Biol.* **142**, 1461-1471.

Durbeej, M. and Campbell, K. P. (2002). Muscular dystrophies involving the dystrophin-glycoprotein complex: an overview of current mouse models. *Curr. Opin. Genet. Dev.* **12**, 349-361.

Durbeej, M., Cohn, R. D., Hrstka, R. F., Moore, S. A., Allamand, V., Davidson, B. L., Williamson, R. A. and Campbell, K. P. (2000). Disruption of the beta-sarcoglycan gene reveals pathogenetic complexity of limb-girdle muscular dystrophy type 2E. *Mol. Cell* **5**, 141-151.

Ervasti, J. M. and Campbell, K. P. (1991). Membrane organization of the dystrophin-glycoprotein complex. *Cell* **66**, 1121-1131.

Ervasti, J. M. and Campbell, K. P. (1993). A role for the dystrophin-glycoprotein complex as a transmembrane linker between laminin and actin. *J. Cell Biol.* **122**, 809-823.

Ervasti, J. M., Ohlendieck, K., Kahl, S. D., Gaver, M. G. and Campbell, K. P. (1990). Deficiency of a glycoprotein component of the dystrophin complex in dystrophic muscle. *Nature* **345**, 315-319.

Ervasti, J. M., Kahl, S. D. and Campbell, K. P. (1991). Purification of dystrophin from skeletal muscle. *J. Biol. Chem.* **266**, 9161-9165.

Guo, L. T., Zhang, X. U., Kuang, W., Xu, H., Liu, L. A., Vilquin, J. T., Miyagoe-Suzuki, Y., Takeda, S., Ruegg, M. A., Wewer, U. M. et al. (2003). Laminin alpha2 deficiency and muscular dystrophy; genotype-phenotype correlation in mutant mice. *Neuromuscul. Disord.* **13**, 207-215.

Helbling-Leclerc, A., Zhang, X., Topaloglu, H., Cruaud, C., Tesson, F., Weissenbach, J., Tome, F. M. S., Schwartz, K., Fardeau, M., Tryggvason, K. et al. (1995). Mutations in the laminin α2-chain gene (LAMA2) cause merosin-deficient congenital muscular dystrophy. *Nat. Genet.* **11**, 216-218.

Hemler, M. E. (2001). Specific tetraspanin functions. *J. Cell Biol.* **155**, 1103-1107.

Hemler, M. E. (2003). Tetraspanin proteins mediate cellular penetration, invasion, and fusion events and define a novel type of membrane microdomain. *Annu. Rev. Cell Dev. Biol.* **19**, 397-422.

Henry, M. D. and Campbell, K. P. (1998). A role for dystroglycan in basement membrane assembly. *Cell* **95**, 859-870.

Henry, M. D., Satz, J. S., Brakebusch, C., Costell, M., Gustafsson, E., Fassler, R. and Campbell, K. P. (2001). Distinct roles for dystroglycan, beta1 integrin and perlecan in cell surface laminin organization. *J. Cell Sci.* **114**, 1137-1144.

Hoffman, E. P., Brown, R. H. and Kunkel, L. M. (1987). Dystrophin: the protein product of the Duchenne muscular dystrophy locus. *Cell* **51**, 919-928.

Holt, K. H., Lim, L. E., Straub, V., Venzke, D. P., Duclos, F., Anderson, R. D., Davidson, B. L. and Campbell, K. P. (1998). Functional rescue of the sarcoglycan complex in the Bio 14.6 hamster using δ-sarcoglycan gene transfer. *Mol. Cell* **1**, 841-848.

Ibraghimov-Beskrovnaya, O., Ervasti, J. M., Leveille, C. J., Slaughter, C. A., Sernett, S. W. and Campbell, K. P. (1992). Primary structure of dystrophin-associated glycoproteins linking dystrophin to the extracellular matrix. *Nature* **355**, 696-702.

Judge, L. M., Haraguchiln, M. and Chamberlain, J. S. (2006). Dissecting the signaling and mechanical functions of the dystrophin-glycoprotein complex. *J. Cell Sci.* **119**, 1537-1546.

Jung, D., Duclos, F., Apostol, B., Straub, V., Lee, J. C., Allamand, V., Venzke, D. P., Sunada, Y., Moomaw, C. R., Leveille, C. J. et al. (1996). Characterization of d-sarcoglycan, a novel component of the oligomeric sarcoglycan complex involved in limb-girdle muscular dystrophy. *J. Biol. Chem.* **50**, 32321-32329.

Kanagawa, M., Michele, D. E., Satz, J. S., Barresi, R., Kusano, H., Sasaki, T., Timpl, R., Henry, M. D. and Campbell, K. P. (2005). Disruption of perlecan binding and matrix assembly by post-translational or genetic disruption of dystroglycan function. *FEBS Lett.* **579**, 4792-4796.

Kuang, W., Xu, H., Vachon, P. H., Liu, L., Loechel, F., Wewer, U. M. and Engvall, E. (1998). Merosin-deficient congenital muscular dystrophy. Partial genetic correction in two mouse models. *J. Clin. Invest.* **102**, 844-852.

Kuo, H. J., Maslen, C. L., Keene, D. R. and Glanville, R. W. (1997). Type VI collagen anchors endothelial basement membranes by interacting with type IV collagen. *J. Biol. Chem.* **272**, 26522-26529.

Lampe, A. K. and Bushby, K. M. (2005). Collagen VI related muscle disorders. *J. Med. Genet.* **42**, 673-685.

Langenbach, K. J. and Rando, T. A. (2002). Inhibition of dystroglycan binding to laminin disrupts the PI3K/AKT pathway and survival signaling in muscle cells. *Muscle Nerve* **26**, 644-653.

Lebakken, C. S., Venzke, D. P., Hrstka, R. F., Consolino, C. M., Faulkner, J. A., Williamson, R. A. and Campbell, K. P. (2000). Sarcospan-deficient mice maintain normal muscle function. *Mol. Cell. Biol.* **20**, 1669-1677.

Levy, S. and Shoham, T. (2005). Protein-protein interactions in the tetraspanin web. *Physiology Bethesda* **20**, 218-224.

Lim, L. E., Duclos, F., Broux, O., Bourg, N., Sunada, Y., Allamand, V., Meyer, J., Richard, I., Moomaw, C., Slaughter, C. et al. (1995). Beta-sarcoglycan: characterization and role in limb-girdle muscular dystrophy linked to 4q12. *Nat. Genet.* **11**, 257-265.

Lynch, G. S., Rafael, J. A., Chamberlain, J. S. and Faulkner, J. A. (2000). Contraction-induced injury to single permeabilized muscle fibers from mdx, transgenic mdx, and control mice. *Am. J. Physiol. Cell Physiol.* **279**, C1290-C1294.

Matsuda, R., Nishikawa, A. and Tanakaa, H. (1995). Visualization of dystrophic muscle fibers in mdx mouse by vital staining with evans blue: evidence of apoptosis in dystrophin-deficient muscle. *J. Biochem.* **118**, 959-964.

McArdle, A., Edwards, R. H. and Jackson, M. J. (1994). Time course of changes in plasma membrane permeability in the dystrophin-deficient mdx mouse. *Muscle Nerve* **17**, 1378-1384.

McNally, E. M., Yoshida, M., Mizuno, Y., Ozawa, E. and Kunkel, L. M. (1994). Human adhalin is alternatively spliced and the gene is located on chromosome 17q21. *Proc. Natl. Acad. Sci. USA* **91**, 9690-9694.

Menke, A. and Jockusch, H. (1991). Decreased osmotic stability of dystrophin-less muscle cells from the mdx mouse. *Nature* **349**, 69-71.

Michele, D. E. and Campbell, K. P. (2003). Dystrophin-glycoprotein complex: post-translational processing and dystroglycan function. *J. Biol. Chem.* **278**, 15457-15460.

Miller, G., Peter, A. K., Espinoza, E., Heighway, J. and Crosbie, R. H. (2006). Over-expression of Microspan, a novel component of the sarcoplasmic reticulum, causes severe muscle pathology with triad abnormalities. *J. Muscle Res. Cell Motil.* **27**, 545-558.

Miyagoe, Y., Hanaoka, K., Nonaka, I., Hayasaka, M., Nabeshima, Y., Arahata, K., Nabeshima, Y. and Takeda, S. (1997). Laminin alpha2 chain-null mutant mice by targeted disruption of the Lama2 gene: a new model of merosin (laminin 2)-deficient congenital muscular dystrophy. *FEBS Lett.* **415**, 33-39.

Miyagoe-Suzuki, Y., Nakagawa, M. and Takeda, S. (2000). Merosin and congenital muscular dystrophy. *Microsc. Res. Tech.* **48**, 181-191.

Nigro, V., Piluso, G., Belsito, A., Politano, L., Puca, A. A., Papparella, S., Rossi, E., Viglietto, G., Esposito, M. G., Abbondanza, C. et al. (1996). Identification of a novel sarcoglycan gene at 5q33 encoding a sarcolemmal 35 kDa glycoprotein. *Hum. Mol. Genet.* **5**, 1179-1186.

Pan, T. C., Zhang, R. Z., Sudano, D. G., Marie, S. K., Bonnemann, C. G. and Chu, M. L. (2003). New molecular mechanism for Ullrich congenital muscular dystrophy: a heterozygous in-frame deletion in the COL6A1 gene causes a severe phenotype. *Am. J. Hum. Genet.* **73**, 355-369.

Peter, A. K. and Crosbie, R. H. (2006). Hypertrophic response of Duchenne and limb-girdle muscular dystrophies is associated with activation of Akt pathway. *Exp. Cell Res.* **312**, 2580-2591.

Petrof, B. J., Shrager, J. B., Stedman, H. H., Kelly, A. M. and Sweeney, H. L. (1993). Dystrophin protects the sarcolemma from stresses developed during muscle contraction. *Proc. Natl. Acad. Sci. USA* **90**, 3710-3714.

Rafael, J. A., Sunada, Y., Cole, N. M., Campbell, K. P., Faulkner, J. A. and Chamberlain, J. S. (1994). Prevention of dystrophic pathology in mdx mice by a truncated dystrophin isoform. *Hum. Mol. Genet.* **3**, 1725-1733.

Rafael, J. A., Cox, G. A., Corrado, K., Jung, D., Campbell, K. P. and Chamberlain, J. S. (1996). Forced expression of dystrophin deletion constructs reveals structure-function correlations. *J. Cell Biol.* **134**, 93-102.

Rafael, J. A., Tinsley, J. M., Potter, A. C., Deconinck, A. E. and Davies, K. E. (1998). Skeletal muscle-specific expression of a utrophin transgene rescues utrophin-dystrophin deficient mice. *Nat. Genet.* **19**, 79-82.

Roberds, S. L., Anderson, R. D., Ibraghimov-Beskrovnaya, O. and Campbell, K. P. (1993). Primary structure and muscle-specific expression of the 50-kDa dystrophin-associated glycoprotein (adhalin). *J. Biol. Chem.* **268**, 23739-23742.

Roberds, S. L., Letrucq, F., Allamand, V., Piccolo, F., Jeanpierre, M., Anderson, R. D., Lim, L. E., Lee, J. C., Tome, F. M. S., Romero, N. B. et al. (1994). Missense mutations in the adhalin gene linked to autosomal recessive muscular dystrophy. *Cell* **78**, 625-633.

Spencer, M. J. and Mellgren, R. L. (2002). Overexpression of a calpastatin transgene in mdx muscle reduces dystrophic pathology. *Hum. Mol. Genet.* **11**, 2645-2655.

Spencer, M. J., Guyon, J. R., Sorimachi, H., Potts, A., Richard, I., Herasse, M., Chamberlain, J., Dalkilic, I., Kunkel, L. M. and Beckmann, J. S. (2002). Stable expression of calpain 3 from a muscle transgene in vivo: immature muscle in transgenic mice suggests a role for calpain 3 in muscle maturation. *Proc. Natl. Acad. Sci. USA* **99**, 8874-8879.

Straub, V., Rafael, J. A., Chamberlain, J. S. and Campbell, K. P. (1997). Animal models for muscular dystrophy show different patterns of sarcolemmal disruption. *J. Cell Biol.* **139**, 375-385.

Straub, V., Duclos, F., Venzke, D. P., Lee, J. C., Cutshall, S., Leveille, C. J. and Campbell, K. P. (1998). Molecular pathogenesis of muscle: degeneration in the δ-sarcoglycan-deficient hamster. *Am. J. Pathol.* **153**, 1623-1630.

Sunada, Y., Bernier, S. M., Kozak, C. A., Yamada, Y. and Campbell, K. P. (1994). Deficiency of merosin in dystrophic dy mice and genetic linkage of laminin M chain gene to dy locus. *J. Biol. Chem.* **269**, 13729-13732.

Taveau, M., Stockholm, D., Spencer, M. and Richard, I. (2002). Quantification of splice variants using molecular beacon or scorpion primers. *Anal. Biochem.* **305**, 227-235.

Tidball, J. G. and Spencer, M. J. (2002). Expression of a calpastatin transgene slows muscle wasting and obviates changes in myosin isoform expression during murine muscle disuse. *J. Physiol.* **545**, 819-828.

Tidball, J. G., Albrecht, D. E., Lokensgard, B. E. and Spencer, M. J. (1995). Apoptosis precedes necrosis of dystrophin-deficient muscle. *J. Cell Sci.* **108**, 2197-2004.

Tillet, E., Wiedemann, H., Golbik, R., Pan, T. C., Zhang, R. Z., Mann, K., Chu, M. L. and Timpl, R. (1994). Recombinant expression and structural and binding properties of alpha 1(VI) and alpha 2(VI) chains of human collagen type VI. *Eur. J. Biochem.* **221**, 177-185.

Weller, B., Karpati, G. and Carpenter, S. (1990). Dystrophin-deficient mdx muscle fibers are preferentially vulnerable to necrosis induced by experimental lengthening contractions. *J. Neurol. Sci.* **100**, 9-13.

Xu, H., Christmas, P., Wu, X.-R., Wewer, U. M. and Engvall, E. (1994). Defective muscle basement membrane and lack of M-laminin in the dystrophic *dy/dy* mouse. *Proc. Natl. Acad. Sci. USA* **91**, 5572-5576.

Yang, B., Ibraghimov-Beskrovnaya, O., Moomaw, C. R., Slaughter, C. A. and Campbell, K. P. (1994). Heterogeneity of the 59-kDa dystrophin-associated protein revealed by cDNA cloning and expression. *J. Biol. Chem.* **269**, 6040-6044.

Yoshida, M. and Ozawa, E. (1990). Glycoprotein complex anchoring dystrophin to sarcolemma. *J. Biochem.* **108**, 748-752.

Zhu, X., Hadhazy, M., Groh, M. E., Wheeler, M. T., Wollmann, R. and McNally, E. M. (2001). Overexpression of gamma-sarcoglycan induces severe muscular dystrophy. Implications for the regulation of sarcoglycan assembly. *J. Biol. Chem.* **276**, 21785-21790.